Repetitive Stresses Generate Osteochondral Lesions in Skeletally Immature Rabbits

Austin V. Stone,*† MD, PhD, Kevin J. Little,‡ MD, David L. Glos,‡ BS, Keith F. Stringer,§ MD, and Eric J. Wall,‡ MD
Investigation performed at the Department of Orthopaedic Surgery, Cincinnati Children's Hospital Medical Center, Cincinnati, Ohio, USA

Background: The origin of juvenile osteochondritis dissecans (OCD) is unknown. Existing experimental animal models of OCD most frequently involve surgically created lesions but do not examine repetitive stress as a possible cause of OCD.

Hypothesis: Repetitive stresses can cause OCD-like lesions in immature animals.

Study Design: Controlled laboratory study.

Methods: Six juvenile rabbits were subjected to repetitive loading forces of approximately 160% body weight to the right hindlimb during five 45-minute sessions per week for 5 weeks. The contralateral limb was the unloaded control. After 5 weeks, rabbits were euthanized and examined with radiographs, micro–computed tomography, and gross and histopathologic analysis.

Results: All 6 rabbits developed osteochondral lesions in loaded limbs on the medial and lateral femoral condyles, while contralateral unloaded limbs did not demonstrate lesions. Loaded limbs developed relative osteopenia in the femoral epiphysis and tibial metaphysis with associated decreased trabecular density. Loaded limbs also demonstrated increased femoral subchondral bone thickness near the lesions. Lesions did not have grossly apparent extensive articular cartilage damage; however, cartilage thickness increased on histology with reduced ossification. Loaded knees demonstrated abundant chondrocyte cloning, limited cartilage fissuring, and a focal loss of cellularity at the articular surface.

Conclusion: Low-grade lesions in human OCD have little gross articular cartilage involvement despite substantial changes to the subchondral bone as shown on magnetic resonance imaging and radiographs. Histopathology findings in this study included cartilage thickening and chondrocyte cloning resembling those of recently published human OCD biopsy studies. Our animal model supports the hypothesis that repetitive stress to immature knees may contribute to the development of human OCD. This model may be useful in understanding the pathophysiology and healing of human OCD.

Clinical Relevance: Repetitive physiologic stress generated changes to the subchondral bone in immature animals without causing extensive articular damage. The similarities of these lesions in gross and histologic appearance with human OCD support repetitive stress as the likely the cause for human OCD.

Keywords: osteochondral; juvenile osteochondritis dissecans; osteochondritis dissecans; subchondral bone; cartilage

Juvenile osteochondritis dissecans (OCD) is an increasingly common source of knee pain in young patients and can lead to osteoarthritis in adolescence and later in life. The cause remains unclear but is thought to be related to repetitive microtrauma and may include secondary ossification disruption, vascular insult, and a degree of genetic predisposition.[2,7,12,14,19,26,44,45] Early-stage OCD involves injury to the subchondral bone and is often without arthroscopically visible articular cartilage damage.[14,24,45] Some of these lesions may fail to heal or may develop articular cartilage damage and require operative treatment.[18,24,45,46] Unresolved OCD lesions that develop in childhood are thought to be responsible for many of the adult cases of OCD,[10] and unhealed OCD may lead to articular cartilage loss with subsequent osteoarthritis.[4,8,30,43] Both nonsurgical and surgical approaches have been employed to treat OCD; however, the treatment efficacy is highly variable.¶ Little evidence supports the current treatments for OCD.[3,15] Since the cause for OCD is elusive and the clinical condition is rare, the development of an animal model for creation, evaluation, and treatment of OCD may make significant contributions to diagnosing and treating existing lesions and subsequently preventing early-onset osteoarthritis.

The American Journal of Sports Medicine, Vol. 44, No. 11
DOI: 10.1177/0363546516654479

¶References 10, 13, 16, 19, 24, 27, 36, 45, 46

Several animal models of OCD are reported. Early animal models involved the creation of OCD via a surgically generated lesions, but this methodology is not compatible with the proposed origin.[1,22,40] More recent investigation into OCD in animal models examined the microvascular compromise and evaluated abnormalities in endochondral ossification.[11,32,34,42,49-52] An animal model using repetitive stress in juvenile knees may aid in the understanding of juvenile OCD (JOCD) and provide an additional platform for testing the aforementioned theories. The purpose of this study was to determine if repetitive physiologic loads would produce subchondral lesions in juvenile rabbits with minimal gross articular surface involvement consistent with an International Cartilage Repair Society (ICRS) type I lesion.

METHODS

A total of 6 skeletally immature New Zealand White rabbits (initial age, 29-36 days; Charles River Laboratories) were subjected to mechanical loading and examination. Rabbits were housed with the mother in standard cages in a 12-hour light/dark cycle for the duration of testing, with appropriate food, water, and enrichment. Rabbits underwent daily evaluation for injury, pain, and discomfort. Injured rabbits were euthanized or withheld from testing until the symptoms receded. Experimental animal care and use were in full compliance with guidelines established by the Cincinnati Children's Hospital Research Foundation Institutional Animal Care and Use Committee, Animal Welfare Act, pertinent state and local laws, Public Health Service policy, National Institutes of Health's guide for care and use of laboratory animals, and the US Interagency of Research Animal Committee Principles.

Repetitive Impulse Loading Device

Controlled variables included loading frequency, displacement, duration of loading, position of limbs (flexion and extension), and which limb was loaded. Measured variables included axial force, rabbit mass, lesion size, and lesion location. The right leg of each rabbit served as the experimental limb, while the left limb served as the control. The control limb was not subjected to any type of testing or modification.

A custom compressive loading device was constructed similar to one used by Serink et al[40] (Figure 1). The device generated a sinusoidal displacement at a frequency of 1 Hz by means of a flywheel attached to an electric motor. A maximum displacement of either 5.0 or 7.5 mm in the flywheel was controlled by interchangeable cams. A loading plate was mounted in line with a load cell (50 lb; model SBO-50; Transducer Techniques) and a spring system. The spring system decreased the effective stiffness of the system to permit fine-tuning of the load profile.

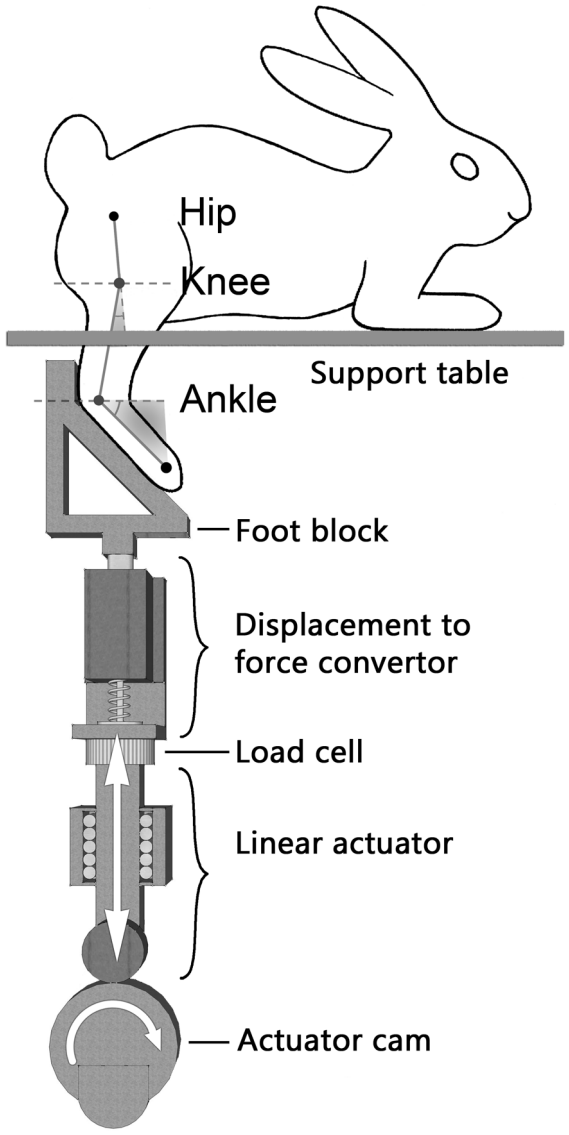

Figure 1. Schematic of the rabbit loading device.

*Address correspondence to Austin V. Stone, MD, PhD, Department of Orthopaedic Surgery, Wake Forest School of Medicine, Medical Center Boulevard, Winston-Salem, NC 27157-1070, USA (email: austinvstonemd@gmail.com).
†Department of Orthopaedic Surgery, Wake Forest School of Medicine, Winston-Salem, North Carolina, USA.
‡Department of Orthopaedic Surgery, Cincinnati Children's Hospital Medical Center, Cincinnati, Ohio, USA.
§Department of Pathology, Cincinnati Children's Hospital Medical Center, Cincinnati, Ohio, USA.

One or more of the authors has declared the following potential conflict of interest or source of funding: Funding for this study was primarily provided by grant support from the Orthopaedic Research and Education Foundation (OREF 07-112, OREF/DePuy 08-029) and the University of Cincinnati University OREF. Additional support was received from an Institutional Clinical and Translational Science Award (National Institutes of Health / National Center for Research Resources 5UL1RR026314 03) and the Charlotte R. Schmidlapp Women's Scholar Program. A.V.S.: Smith & Nephew LLC (research support). E.J.W.: Cincinnati Children's Physician-Hospital Organization (board or committee member), OrthoPediatrics (paid consultant), PRISM (board or committee member), ROCK Group (board or committee member), SpineForm (other financial or material support, research support, stock or stock options, unpaid consultant).

Repetitive Impulse Loading of Rabbits

Rabbits were secured in the prone position to a table top attached to the loading mechanism. The right hindlimb of the rabbit was placed through a hole in the table while the left hindlimb was tucked under the body with the knee and hip flexed in a normal resting position. Vet wrap (Coban; 3M) was used to secure the right foot to the loading plate holding the foot at an angle of 45° (Figure 1). The right thigh was secured against a block with a Velcro strap. The right knee was maintained in 15° of flexion (Figure 1). An aluminum bracket with adjustable threaded rods holding a custom Orthoplast (Johnson & Johnson) mold was used to minimize movement of the hips and secure the rabbit to the table to ensure effective force delivery from the loading device to the knee.

Maximum displacement was 5.0 mm for weeks 1 and 2 and adjusted to 7.5 mm for weeks 3 to 5 to increase the total force produced. Daily calibrations of the load cell with multiple calibration blocks (mass: 2.58, 2.27, 9.18 kg) were conducted before animal testing to determine the zero point and calibration ratio for analysis.

Rabbits were subjected to a sinusoidal loading session for 45 minutes per day, 5 days per week for a total of 5 weeks. Before each loading session, rabbit mass and loading specifications were recorded. Isoflurane gas was used for anesthesia for the duration of loading. Immediately after the loading sessions, rabbits were administered a 0.1-mL intramuscular injection of buprenorphine (Buprenex; Reckitt Benckiser Pharmaceuticals) for analgesia. Rabbits were then placed in a warm incubator and examined. After complete recovery, rabbits were returned to their cage.

Applied force was measured with a load cell (50 lb; model SBO-50) and data acquisition system (Agile-Link v 1.3.9; MicroStrain Inc). Measurements were collected at loading session time points 0, 15, 30, and 45 minutes during each day of testing. Time point data collection cycles were 38 seconds in duration, and each acquired approximately 66,000 samples. Load histories were converted into the frequency domain by fast Fourier transform, low pass filtered, and converted back to the time domain with an inverse fast Fourier transform (GNU Octave 3.0.3 with protocol from John W. Eaton et al, University of Wisconsin, Department of Chemical Engineering). Maximum and minimum peaks were found through peak detection. Force, smoothed force, maximum force, minimum force, and dynamic force were determined.

Radiographic Analysis

Weekly anteroposterior and lateral radiographs of the rabbit hindlimbs were obtained. Radiographs were examined for signs of osteochondral lesions and other abnormalities or injuries and digitized (Nikon D100 digital camera with a 60-mm Micro Nikkor lens).

After the 5 weeks of testing, rabbits were euthanized under anesthesia with an injection of pentobarbital (Fatal-Plus; Vortech Pharmaceuticals). After euthanasia, both hindlimbs were disarticulated at the femoral head and the knee joints preserved. The limbs were immediately placed on ice for imaging with micro–computed tomography (micro-CT), followed by tissue processing for histologic analysis.

Micro-CT Analysis

Rabbit knees were scanned with a MicroCAT II micro-CT scanner (ImTek) in the axial plane at an isotropic thickness of 31 μm (144 μA, 59 kVp; image matrix, 640 × 640 pixels). Matrix images were reformatted into standard sagittal and coronal planes with 3-dimensional (3D) reconstructions (Amira v5.4; Visage Imaging). Images were assessed for physeal widening, physeal fracture, and subarticular changes. Lesion widths and lengths were measured with the 3D measurement tool on the subchondral bone surface on 3D renderings to most closely approximate lesion size. The respective coronal or sagittal slice was juxtaposed with the 3D image during measuring to ensure accurate endpoints. Surface area was then calculated.

Lesion location and volume were found with the isosurface, the visualized bone boundary of the 3D reconstruction after application of a threshold of 950 Hounsfield units (HU), based on published guidelines.[6] Lesions were classified as being on the medial or lateral condyle. Lesion volume was determined by multiplying the length, width, and depth. An orthogonal slice at the intersection of the axis of the length and width was used to find lesion depth. Femoral epiphyses and tibial metaphyses were extracted from the full scan. Bone volume and density were determined for full and threshold (>950 HU, femoral epiphysis; >875 HU, tibial metaphysis) image sets to derive, respectively, total bone volume and density and the mineralized bone volume and density.[6] The tibial region of interest was based on the normalized height of the metaphysis, two-thirds of the distance between the proximal metaphyseal bone to the proximal border of the medullary canal. Measured outcome variables were total volume (V_T), mineralized bone volume (V_B), bone volume fraction ($100 \times [V_B/V_T]$), total density (ρ_T), and mineralized bone density (ρ_B). The number of sections used for the metaphyseal region of interest were 149 ± 14 and 146 ± 15 for left and right limbs, respectively. To test for statistical differences, 2-tailed paired t tests were used, followed by the Bonferroni post hoc correction ($\alpha = 0.05/4$).

Histopathologic Analysis

Extracted bones were returned on ice after micro-CT scanning. Each knee was opened and articular cartilage exposed for photography with a Nikon D100 digital camera and 60-mm Micro Nikkor lens (Nikon, Tokyo, Japan). Gross cartilage lesions were graded with the ICRS classification system 2000 for OCD lesions. The articular surface was preserved and the joints fixed in 4% paraformaldehyde (Electron Microscopy Services) in phosphate-buffered saline at 4°C. After fixation, specimens were decalcified (10% EDTA [pH 7.4] at 25°C), sectioned in the sagittal plane, dehydrated in ethanol, and embedded in paraffin. Histology sections (4 μm) were stained with hematoxylin and eosin or trichrome stain. Slides were photographed

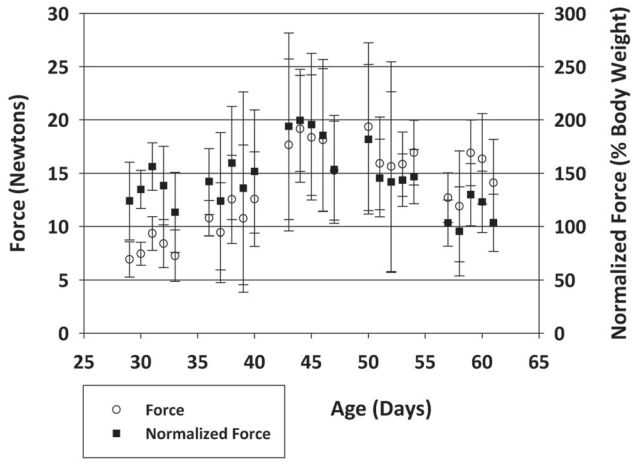

Figure 2. Time course of loading force: measured loading force and force normalized to body weight. Force as a function of body weight remained within physiologic limits.

with a Zeiss Axioskop microscope (Zeiss Optronics) equipped with a Spot RT3 digital camera (Spot Diagnostics). Stained sections were analyzed for the presence of trabecular microfractures, microhematomas, articular cartilage damage, and physeal damage.

RESULTS

Rabbit Growth and Development

Four of the 6 rabbits completed 5 weeks of testing, while 2 rabbits completed 4 weeks of testing. During the 5 weeks of testing, rabbits gained a total of 630 ± 20 g at a rate of 28 ± 5.0 g per day. All rabbits in the testing group grew at a similar rate, within previously published normal values[28,31] and with no evidence of failure to thrive for the duration of the study. Rabbits appeared to tolerate testing well and remained active in their cages. All rabbits demonstrated mild limb avoidance beginning the first week of testing.

One rabbit had a fracture before loading and was immediately euthanized. The rabbit was not photographed or graded. In the fifth week of testing, 1 rabbit developed a Salter-Harris II physeal fracture and was withheld from testing for 2 days and euthanized. Three rabbits had evidence of physeal widening and healing callus formation by micro-CT; however, the 4 remaining rabbits completed all 5 weeks of testing.

Application of Force

Preload tension and compression were minimized during rabbit adjustments; however, some rabbits experienced slight variations in the preload tension or compression secondary to movement and settling into the loading device.

Loaded limbs in rabbits received an average load per session of 124% ± 38% body weight. Rabbits experienced the greatest load as a percentage of body weight during the third week of testing, after the change from the 5.0- to 7.5-mm cam, with mean changes in load of 148% ± 44% body weight (Figure 2). No rabbit experienced a load >275% body weight. Mean absolute loads and loads as a percentage of body weight were similar among rabbits during the same week of testing.

Radiographic Analysis of Osteochondral Lesions

Rabbits underwent weekly radiographic evaluation of the experimental and contralateral control hindlimbs, which did not reveal grossly evident subchondral bone lesions. Subsequent micro-CT evaluation after euthanasia demonstrated at least 1 osteochondral lesion in each loaded limb, while contralateral limbs did not have any defects. Subchondral defects in the medial condyle were greater than those in the lateral condyle. All 6 rabbits developed lesions on the medial femoral condyle (MFC) of the loaded limb, while 5 of 6 rabbits developed lesions on the lateral femoral condyle (LFC) of the loaded limb. The mean ± SEM surface areas of MFC and LFC lesions were 6.3 ± 2.0 mm^2 and 5.0 ± 1.7 mm^2, respectively. Lesions were present on the inferolateral aspect of the MFC and the inferomedial aspect of the LFC.

Two-dimensional micro-CT also revealed qualitatively decreased epiphyseal trabecular density in loaded limbs as compared with control limbs in terms of the entire epiphysis. Loaded limbs demonstrated subchondral bone thickening beneath the cartilage lesions (Figure 3). Contralateral controls exhibited no evidence of reactive subchondral bone changes. Control limb micro-CT images appeared grossly similar among all rabbits with no qualitative changes in signal intensity (Figure 3).

Mineralized bone volume in experimental femoral epiphyses was 23% less than paired controls: experimental limb, 371 mm^3 (95% CI: 277-465 mm^3); control limb, 481 mm^3 (95% CI: 409-553 mm^3; $P = .002$) (Figure 4A). Total epiphyseal volume was not different between control and experimental joints ($P = .84$) (Figure 4A). Bone volume fraction of the experimental limb was 24% less than the control limb: 36% (95% CI: 30%-41%) versus 47% (95% CI: 45%-49%; $P = .002$) (Figure 4C). Total epiphyseal bone density was 12% lower in experimental knees than in paired controls: 815 HU (95% CI: 767-862 HU) versus 925 HU (95% CI: 910-941 HU; $P < .001$) (Figure 4E). Mineralized bone density in experimental knees was also lower than control: 1212 mm^3 (95% CI: 1174-1250 mm^3) versus 1256 mm^3 (95% CI: 1227-1284 mm^3; $P = .001$) (Figure 4E).

Tibial metaphyseal mineralized bone volumes were decreased in loaded limbs (229 mm^3; 95% CI: 185-272 mm^3) versus control limbs (322 mm^3; 95% CI: 270-374 mm^3; $P < .001$) (Figure 4B). Total metaphyseal mineralized bone volumes were also decreased in loaded limbs (350 mm^3; 95% CI: 300-400 mm^3) as compared with controls (401 mm^3; 95% CI: 331-472 mm^3; $P = .016$) (Figure 4B). Bone volume fractions were likewise significantly decreased in loaded limbs: 65% (95% CI: 59%-72%) versus 81% (95% CI: 75%-86%; $P = .006$) (Figure 4D). Reductions, as compared with the control side, for mineralized bone volume and bone volume fraction were 29% and 19%, respectively. Control limb mineralized densities were greater than loaded tibial

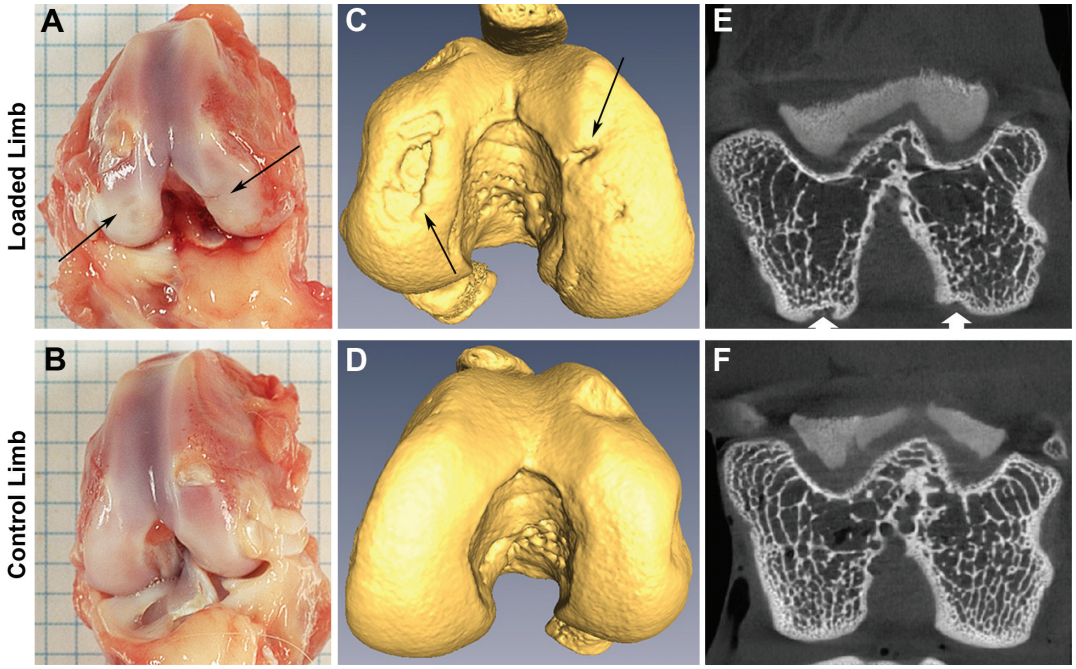

Figure 3. Representative (A, B) gross pathologic abnormalities and corresponding (C, D) micro–computed tomography reconstructions and (E, F) slices from the loaded and contralateral control limbs of a single rabbit. Arrows point to the osteochondral lesions.

metaphyseal densities: 1052 HU (95% CI: 1039-1065 HU) for controls and 1027 HU (95% CI: 1012-1042 HU) for experimental (P = .012; Figure 4F). Total tibial metaphyseal density was greater in controls (993 HU; 95% CI: 964-1023 HU) as compared with loaded limbs (913 HU; 95% CI: 878-948 HU; P = .005) (Figure 4F). The reductions, as compared with controls, in mineralized bone density and total bone density were 2% and 8%, respectively.

Gross Analysis of Cartilage Defects

Rabbits did not have grossly apparent extensive articular cartilage involvement in loaded legs. Gross pathologic analysis demonstrated cartilaginous defects of ICRS types I and II on the MFC on all 5 graded rabbits and ICRS type I lesions on the LFC of 4 of 5 graded rabbits. No defects of type III or higher were present on the loaded limbs. All MFC lesions were located on the lateral aspect of the MFC and the inferior aspect of the LFC. Cartilage damage was not evident on the contralateral control limbs (Figure 3). The aforementioned rabbit that sustained a fracture while in its cage was not photographed before histology preparation and was consequently not graded.

Histopathologic Analysis of Defects

Histopathologic analysis identified multiple structural changes in the cartilage of loaded limbs as compared with control limbs. In the discrete areas of change in loaded limbs, maximal cartilage thickness doubled (mean, 1.0 mm) (Figure 5B) when compared with the control limb at the corresponding location (mean, 0.5 mm) (Figure 5A). Joint surface irregularities, including horizontal cracks or vertical fissure-like clefts, were present in 2 loaded knees (Figure 5, C and D), and focal articular surface depressions or elevations were identified in all loaded knees (Figure 5, C and F). Geographic nuclear dropout was also present in those areas, as evidenced by loss of basophilic (blue) staining there (Figure 5E). Chondrocyte cloning was identified in all cases, wherein nests of chondrocytes cluster abnormally in ball-like formations (Figure 5F).[38,47,48] Trabecular structure was not quantified on histology, since it was analyzed on micro-CT; however, it was qualitatively decreased in the femoral epiphysis. All contralateral control limbs were normal in histologic appearance.

DISCUSSION

In the present study, repetitive compressive loading of the knee joint produced osteochondral lesions in the skeletally immature rabbit. An important goal of this study was to produce lesions with repetitive microtrauma and without extensive damage to the articular cartilage unlike acute trauma models. The growth patterns suggest that rabbit nutrition was adequate and that the physeal/osteochondral lesions sustained were not severe enough to cause failure to thrive. Loads applied to the rabbit knee were well within physiologic limits that might be seen with frequent and continuous activity. Previous literature has suggested that axial loads do not result in high variations in growth but

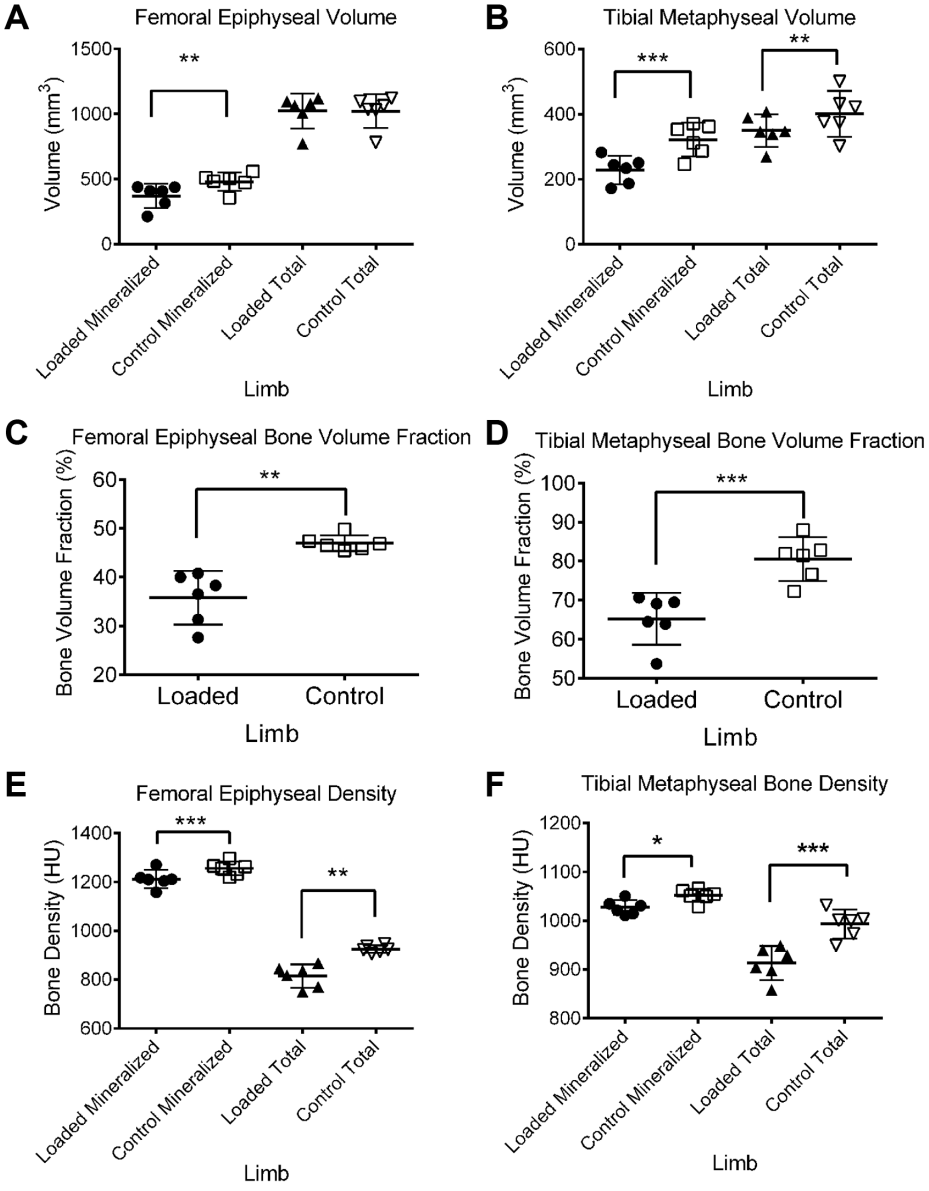

Figure 4. Quantitative radiographic analysis of loaded and control femoral epiphyses and tibial metaphyses. (A) Femoral epiphyseal volume. (B) Tibial metaphyseal bone volume. (C) Femoral epiphyseal bone volume fraction. (D) Tibial metaphyseal bone volume fraction. (E) Femoral epiphyseal bone density. (F) Tibial metaphyseal bone density. Each data point is plotted in the scatter plots, with the horizontal line delineating the mean and the error bars representing the 95% CI. Statistically significant difference: $*P < .05$. $**P < .01$. $***P < .001$. HU, Hounsfield units.

may be correlated with decreased anterior growth.[29] Our rabbit growth did not appear to be affected by loading and was both internally consistent and consistent within published results.[28,31] Maximum loads did not exceed 275% of the rabbit body weight, and means remained within the range of 100% to 200% body weight. The ability to form lesions through low-level repetitive force is congruent with a proposed cause of OCD and an important step forward in developing an animal model for OCD lesions in the developing skeleton.

Previous animal studies for growth plate injury and osteochondral defects offered some insight into the cause of OCD. Drilled lesions significantly damage the articular cartilage and produce a unique pathologic fracture inconsistent with the proposed development of OCD in humans.[1,9,44,48] A repetitive stress model via hyperextension of the adult canine knee successfully generated an OCD-like lesion[39]; however, the rate of hyperextension (7-mm displacement at 1400 revolutions per minute) and the closed canine physes did not offer substantial insight

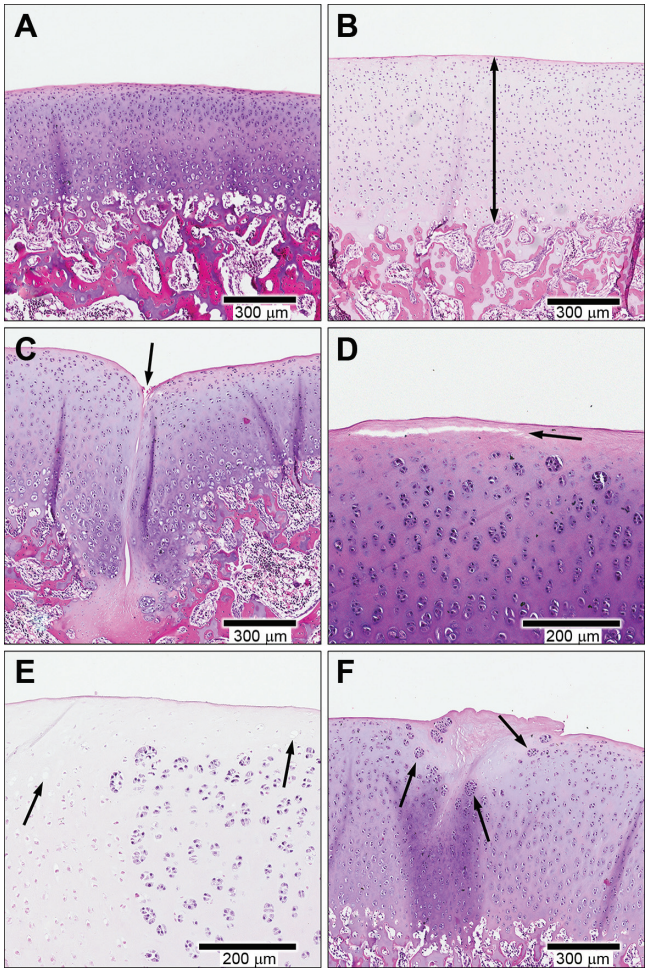

Figure 5. Histopathologic analysis identified multiple structural changes in the cartilage of loaded limbs versus control limbs. (A) Normal control histology. (B) Discrete areas of change in loaded limbs had a maximum cartilage thickness (distance between arrowheads) twice that of the control limb. (C, D) Joint surface irregularities, including cracks and vertical fissure-like clefts (arrow), and focal articular surface depressions or elevations (arrow) in most animals. (E) Nuclear dropout present in loaded limbs (arrows). (F) Chondrocyte cloning (arrows).

into JOCD formation. An OCD-like lesion was created in the skeletally mature rabbit femorotibial joint through use of repetitive compression, which suggests a significant role of repetitive trauma in OCD formation.[40] Later observations[12,17,23] were also consistent with previous repetitive trauma models.[39,40] Our modifications of the published model[40] more tightly regulated the application of force and provided detailed analysis in the context of a healthy skeletally immature rabbit.

The location of the lesions on the MFC was similar to the location of human OCD lesions described by Aichroth[2] and Hefti et al[21] and reviewed by Wall and Von Stein[45] and, more recently, by Edmonds and Polousky.[14] Rabbit lesions were consistently produced on the MFCs, with frequent appearance of lesions of the LFCs. This lesion distribution suggests that the limbs were reliably loaded and followed a pattern of injury similar to patterns seen in humans.[14,21] Furthermore, the radiographic evidence of subchondral bone sclerosis and alterations in the trabeculae was consistent with changes seen in an established genetic-osteochondral defect foal model.[33] We identified that excessive repetitive stresses significantly decreased both bone volume and bone density in the femoral epiphyses of skeletally immature knees. Our model supports the concept that excessive numbers of loading cycles on juvenile joints may compromise the structural integrity of the subchondral bone, which may lead to articular cartilage fissure and failure. In human JOCD histopathology, increased osteoid and fibrous tissue in the region was a common finding in ICRS OCD I lesions, and trabecular structure thinned with lesion progression.[25] The decrease in mineralized bone and the alteration of trabecular patterns correlate to reported histopathology of human JOCD lesions.[25,53] This mechanism is congruent with clinical findings of a well-preserved articular surface at early arthroscopy until subchondral bone loss or fracture.[25,53]

The significant alterations in tibial metaphyseal bone were an unexpected finding. We expected that mineralized bone volume, bone volume fraction, and mineralized bone density would remain unchanged; however, mineralized bone volume and bone volume fraction, as well as mineralized and total bone density, were decreased in the tibial metaphysis of the experimentally loaded limbs as compared with contralateral controls. The more diffuse, albeit mild, osteopenia suggests that protective weightbearing on the loaded limbs may have decreased bone density of the entire limb. The differences in bone volume and density may also be a result of a combination of repetitive loading and reduced limb use or other factors, such as physeal injury. In comparison with the prior results of the femoral epiphysis, the bone volumes of the tibial metaphysis were lower, but the bone densities of the tibia were greater. It is possible that reducing the force used to load the limbs could result in increased tibial bone stress as a result of bone remodeling; however, our study did not examine multiple loading forces.

Cartilage involvement was more extensive on histologic examination than grossly apparent. Cloning of chondrocytes, focal attenuation of cartilage with subchondral bone interdigitation, thickening of cartilage, and cell death were present. A study of OCD lesion histology found evidence of hypertrophied cartilage in biopsy specimens of ICRS OCD I and OCD II lesions, with chondrocyte cloning and articular cartilage microfractures.[48] Chondrocyte cloning and epiphyseal cartilage thickening were also identified on JOCD biopsy histopathology by Zbojniewicz et al.[53]

All loaded limbs demonstrated histologic evidence of focal cartilage thickening and abundant chondrocyte cloning. These findings parallel those in a recent study of human surgical biopsies of articular cartilage in a series of 8 patients with JOCD, which found increased cartilage thickness in half of patents and chondrocyte cloning.[48] Increased thickness of cartilage was commonly identified in a study of detached OCD lesions in adults,[5] and chondrocyte cloning was found in veterinary cases of knee OCD.[38] In human JOCD specimens, cartilage appearance varies from normal to irregular and frankly degenerative.[41]

Sites of frank separation and microfractures at the deep layer of articular cartilage were commonly identified in the adolescent human patients of Yonetani et al,[48] which were not detected in our loaded rabbit limbs. It is possible that the human surgical specimens were at a more advanced stage of injury and may be detected in more severe injuries not generated in our initial repetitive stress model. Chondrocyte clones are seen in other conditions of the knee, such as osteoarthritis.[47] Chondrocytes bordering impacted cartilage in an in vitro study[34] showed loss of spatial organization immediately after acute trauma, and similar changes in our loaded cartilage suggest that matrix degradation may lead to microscopic cartilage involvement. Another recent study examined the articular cartilage response to growth plate injury in rats.[37] Evidence of cartilage irregularities included decreased anisotropy, loss of columns, and formation of cellular cloning and hypocellularity.[37] Articular cartilage changes were considered to be a consequence of growth plate injury and may be attributed to disruption of local growth factor pathways and altered remodeling. It is interesting to note congruencies between the present study's histologic findings and those demonstrated after rat growth plate injury; however, we could not establish a clear link between physeal injury and the articular remodeling identified in our study. Two rabbits in our study demonstrated evidence of physeal overload indicated by the physeal widening, but the altered radiographic appearance of the physis was not present in all with articular cartilage changes. In human JOCD, injury to the secondary physis of the epiphysis was suggested as a cause with progressive subchondral involvement.[26] Future investigation in this animal model may yield additional insight into involvement of the primary or secondary physis and may be more closely tied to the structural alterations of the subchondral bone and articular cartilage.

Evidence of underlying chondromalacia was apparent on gross examination immediately after harvest with a standard camera but was more pronounced when viewed after decalcification under the magnification of a dissecting scope with ring-light illumination. Postharvest photographs were used for ICRS cartilage grading, since lighting and magnification conditions more closely resembled conditions during arthroscopic evaluation in humans. The changes observed on gross pathologic examination do not provide clear evidence of the timing and progression of the lesion formation. The literature is controversial if lesions have (1) early cartilage involvement with progression to more extensive subchondral involvement or (2) early subchondral injury that later involves the articular surface as the injury becomes more extensive. The latter progression would be more characteristic of the proposed development of human OCD lesions. Subchondral bone necrosis was frequently reported in human JOCD detached fragment biopsies, although the proposed origin varied among studies.[41] Recent histologic evaluation of human JOCD lesions demonstrates evidence of active but failing repair responses in and adjacent to the lesions and no evidence of avascular necrosis.[25] Krause et al[25] identified increased osteoblast activity in ICRS OCD I lesions, while ICRS OCD II and III lesions demonstrated fibrocartilaginous tissue with high vascularity at the peripheral and juxta-articular regions of interest. The histopathologic findings of Krause et al were congruent with recently reported JOCD imaging and histopathology specimens that identified marrow edema and unossified epiphyseal cartilage thickening without frequent focal bone necrosis.[53] Fibrovascular tissue was present in all patient biopsy specimens.[53] Despite the frequency of our chondral surface lesions, the micro-CT findings and the histopathology findings in the rabbit OCD model demonstrate substantial similarities and support an origin other than pure avascular necrosis.

While the histopathology of the lesions generated in our study did not demonstrate frank evidence of avascular necrosis, the focal chondral thickening, chondrocyte loss, and subchondral bone loss may be congruent with a compromise of the endochondral ossification described in the veterinary literature.[11,32,34,50,51] An insult (acute or repetitive) to the vasculature supporting endochondral ossification can result in focal necrotic epiphyseal cartilage.[11,32,34,35,50] This microvascular insult can result in compromise of the structural integrity of the surrounding cartilage and subchondral bone.[32,51] Our findings of focal necrosis and subchondral bone loss could be the result of a microvascular injury not detected in our study. It is certainly possible that a microvascular insult from repetitive loading could occur and have an added detrimental effect on the local structural integrity. Future alterations in our loading protocol may further minimize articular surface damage and better elucidate the subchondral bone damage.

While the current study has many data favoring the development of an accurate animal model, it carries limitations. Histopathology was also performed in a qualitative manner and did not evaluate the molecular and microvascular alterations that could contribute to osteochondral abnormalities. It is possible that repetitive mechanical trauma to an immature knee could cause small vessel disruption in the condyle. It is not possible to delineate any changes in vascularity of the subchondral bone and growth plate with noncontrasted micro-CT; however, future studies may incorporate intravascular contrast to elucidate vascular injury in OCD formation.[33] Immunohistochemistry was not performed at this time but will be a component of future investigation to identify alterations in protein expression and molecular signaling that precede structural changes evident on histology. The translational applicability of this overuse protocol to repetitive loading of juvenile rabbit knees is currently limited by analysis of a single time point and loading parameter set. Modifications to the system may now be based on quantitative baseline bone densities. As a consequence of these limitations, future studies may examine a variety of loads and at >1 age group to better mimic the clinical conditions that may lead to JOCD. Future studies may address this limitation by varying the magnitude and duration of the loading protocol. Since all knees developed ICRS type I to II cartilage surface changes, a lesser loading force should still result in osteochondral lesions with less chondral surface damage to better replicate an arthroscopic stage I lesion

with visually normal articular cartilage and subchondral bone changes. A lesser force should also minimize the risk of physeal injury. Despite the model's limitations, our study successfully developed anatomically appropriate osteochondral lesions through physiologically relevant repetitive stress. While rabbit knees experience different biomechanical stress during the hopping cycle than human knees do during ambulation cycles,[20] we believe that the size of the rabbit knee and its growth patterns make the animal model favorable for studying OCD lesions.

This repetitive loading strategy utilizes a novel approach to creating osteochondral lesions in the juvenile skeleton. An effective loading apparatus was developed to generate repetitive physiologic stress on the knee joint. The loading procedure is effective without causing failure to thrive in the young rabbit. Repetitive physiologic loads generated osteochondral lesions and were confirmed by micro-CT and gross and histopathologic examination. The findings suggest similarities to human osteochondral lesions and, specifically, recent evidence of histopathologic findings in human OCD. Our findings support the concept that in young children, daily repetitive activities that greatly exceed physiologic levels in number and duration, even at physiologically normal load magnitudes, may be a cause of osteochondral injuries that result in reduced formation of trabecular and subchondral bone that supports the articular cartilage. This animal model of osteochondral lesions may elucidate the cause of JOCD, and development of this animal model provides a promising platform for investigation into the underlying cause of repetitive stress injury and the healing or failed repair response of the pediatric skeleton. Ultimately, the model may be used to develop treatment strategies that offer clinical translation for improved evidence-based interventions to reduce symptomatic lesions and the risk of osteoarthritis in the active pediatric patient.

ACKNOWLEDGMENT

The authors gratefully acknowledge the technical expertise and critical review from Donita I. Bylski-Austrow, PhD, and Shital Parikh, MD, of Cincinnati Children's Hospital Medical Center. The authors also thank John Pearce, PhD, Scott Dunn, Zachary R. Sheppard, Allison M. Gregg, and Aron Bercz for their technical support.

REFERENCES

1. Aichroth P. Osteochondral fractures and their relationship to osteochondritis dissecans of the knee: an experimental study in animals. *J Bone Joint Surg Br*. 1971;53:448-454.
2. Aichroth P. Osteochondritis dissecans of the knee: a clinical survey. *J Bone Joint Surg Br*. 1971;53:440-447.
3. American Academy of Orthopaedic Surgeons. *Clinical Practice Guideline on the Diagnosis and Treatment of Osteochondritis Dissecans*. Rosemont, IL: American Academy of Orthopaedic Surgeons; 2010.
4. Anderson AF, Pagnani MJ. Osteochondritis dissecans of the femoral condyles: long-term results of excision of the fragment. *Am J Sports Med*. 1997;25:830-834.
5. Barrie HJ. Hypertrophy and laminar calcification of cartilage in loose bodies as probable evidence of an ossification abnormality. *J Pathol*. 1980;132:161-168.
6. Bouxsein ML, Boyd SK, Christiansen BA, et al. Guidelines for assessment of bone microstructure in rodents using micro-computed tomography. *J Bone Miner Res*. 2010;25:1468-1486.
7. Bradley J, Dandy DJ. Osteochondritis dissecans and other lesions of the femoral condyles. *J Bone Joint Surg Br*. 1989;71:518-522.
8. Bradley J, Dandy DJ. Results of drilling osteochondritis dissecans before skeletal maturity. *J Bone Joint Surg Br*. 1989;71:642-644.
9. Braman JP, Bruckner JD, Clark JM, et al. Articular cartilage adjacent to experimental defects is subject to atypical strains. *Clin Orthop Relat Res*. 2005;430:202-207.
10. Cahill BR. Osteochondritis dissecans of the knee: treatment of juvenile and adult forms. *J Am Acad Orthop Surg*. 1995;3:237-247.
11. Carlson CS, Cullins LD, Meuten DJ. Osteochondrosis of the articular-epiphyseal cartilage complex in young horses: evidence for a defect in cartilage canal blood supply. *Vet Pathol*. 1995;32:641-647.
12. Douglas G, Rang M. The role of trauma in the pathogenesis of the osteochondroses. *Clin Orthop Relat Res*. 1981;158:28-32.
13. Edmonds EW, Albright J, Bastrom T, et al. Outcomes of extra-articular, intra-epiphyseal drilling for osteochondritis dissecans of the knee. *J Pediatr Orthop*. 2010;30:870-878.
14. Edmonds EW, Polousky J. A review of knowledge in osteochondritis dissecans: 123 years of minimal evolution from konig to the rock study group. *Clin Orthop Relat Res*. 2013;471:1118-1126.
15. Edmonds EW, Shea KG. Osteochondritis dissecans: editorial comment. *Clin Orthop Relat Res*. 2013;471:1105-1106.
16. Eismann EA, Pettit RJ, Wall EJ, et al. Management strategies for osteochondritis dissecans of the knee in the skeletally immature athlete. *J Orthop Sports Phys Ther*. 2014;44:665-679.
17. Ekman S, Carlson CS. The pathophysiology of osteochondrosis. *Vet Clin North Am Small Anim Pract*. 1998;28:17-32.
18. Flynn JM, Kocher MS, Ganley TJ. Osteochondritis dissecans of the knee. *J Pediatr Orthop*. 2004;24:434-443.
19. Green WT, Banks HH. Osteochondritis dissecans in children. *J Bone Joint Surg Am*. 1953;35:26-47.
20. Gushue DL, Houck J, Lerner AL. Rabbit knee joint biomechanics: motion analysis and modeling of forces during hopping. *J Orthop Res*. 2005;23:735-742.
21. Hefti F, Beguiristain J, Krauspe R, et al. Osteochondritis dissecans: a multicenter study of the european pediatric orthopedic society. *J Pediatr Orthop B*. 1999;8:231-245.
22. Hidaka S, Sugioka Y, Kameyama H. Pathogenesis and treatment of osteochondritis dissecans: an experimental study on chondral and osteochondral fractures in adult and young rabbits. *Nihon Seikeigeka Gakkai Zasshi*. 1983;57:329-339.
23. Kincaid SA, Lidvall ER. Observations on the postnatal morphogenesis of the porcine humeral condyle and the pathogenesis of osteochondrosis. *Am J Vet Res*. 1983;44:2095-2103.
24. Kocher MS, Tucker R, Ganley TJ, et al. Management of osteochondritis dissecans of the knee: current concepts review. *Am J Sports Med*. 2006;34:1181-1191.
25. Krause M, Lehmann D, Amling M, et al. Intact bone vitality and increased accumulation of nonmineralized bone matrix in biopsy specimens of juvenile osteochondritis dissecans: a histological analysis. *Am J Sports Med*. 2015;43:1337-1347.
26. Laor T, Zbojniewicz AM, Eismann EA, et al. Juvenile osteochondritis dissecans: is it a growth disturbance of the secondary physis of the epiphysis? *AJR Am J Roentgenol*. 2012;199:1121-1128.
27. Lebolt JR, Wall EJ. Retroarticular drilling and bone grafting of juvenile osteochondritis dissecans of the knee. *Arthroscopy*. 2007;23:794, e1-e4.
28. Lerner AL, Kuhn JL. Characterization of regional and age-related variations in the growth of the rabbit distal femur. *J Orthop Res*. 1997;15:353-361.
29. Lerner AL, Kuhn JL, Hollister SJ. Are regional variations in bone growth related to mechanical stress and strain parameters? *J Biomech*. 1998;31:327-335.

30. Linden B. Osteochondritis dissecans of the femoral condyles: a long-term follow-up study. *J Bone Joint Surg Am*. 1977;59:769-776.
31. Masoud I, Shapiro F, Kent R, et al. A longitudinal study of the growth of the New Zealand white rabbit: cumulative and biweekly incremental growth rates for body length, body weight, femoral length, and tibial length. *J Orthop Res*. 1986;4:221-231.
32. McCoy AM, Toth F, Dolvik NI, et al. Articular osteochondrosis: a comparison of naturally-occurring human and animal disease. *Osteoarthritis Cartilage*. 2013;21:1638-1647.
33. Olstad K, Cnudde V, Masschaele B, et al. Micro-computed tomography of early lesions of osteochondrosis in the tarsus of foals. *Bone*. 2008;43:574-583.
34. Olstad K, Hendrickson EHS, Carlson CS, et al. Transection of vessels in epiphyseal cartilage canals leads to osteochondrosis and osteochondrosis dissecans in the femoro-patellar joint of foals; a potential model of juvenile osteochondritis dissecans. *Osteoarthritis Cartilage*. 2013;21:730-738.
35. Olstad K, Ytrehus B, Ekman S, et al. Epiphyseal cartilage canal blood supply to the tarsus of foals and relationship to osteochondrosis. *Equine Vet J*. 2008;40:30-39.
36. Parikh SN, Allen M, Wall EJ, et al. The reliability to determine ''healing'' in osteochondritis dissecans from radiographic assessment. *J Pediatr Orthop*. 2012;32:e35-e39.
37. Quintana-Villamandos MB, Sanchez-Hernandez JJ, Delgado-Martos MJ, et al. Evolutional patterns of articular cartilage following growth plate injury in rats. *J Orthop Sci*. 2009;14:646-651.
38. Ralphs SC. Bilateral stifle osteochondritis dissecans in a cat. *J Am Anim Hosp Assoc*. 2005;41:78-80.
39. Rehbein F. [The origin of osteochondritis dissecans]. *Langenbecks Arch Klin Chir Ver Dtsch Z Chir*. 1950;265:69-114.
40. Serink MT, Nachemson A, Hansson G. The effect of impact loading on rabbit knee joints. *Acta Orthop Scand*. 1977;48:250-262.
41. Shea KG, Jacobs JC Jr, Carey JL, et al. Osteochondritis dissecans knee histology studies have variable findings and theories of etiology. *Clin Orthop Relat Res*. 2013;471:1127-1136.
42. Tóth F, Nissi MJ, Ellermann JM, et al. Novel application of magnetic resonance imaging demonstrates characteristic differences in vasculature at predilection sites of osteochondritis dissecans. *Am J Sports Med*. 2015;43:2522-2527.
43. Twyman RS, Desai K, Aichroth PM. Osteochondritis dissecans of the knee: a long-term study. *J Bone Joint Surg Br*. 1991;73:461-464.
44. Uozumi H, Sugita T, Aizawa T, et al. Histologic findings and possible causes of osteochondritis dissecans of the knee. *Am J Sports Med*. 2009;37:2003-2008.
45. Wall E, Von Stein D. Juvenile osteochondritis dissecans. *Orthop Clin North Am*. 2003;34:341-353.
46. Wall EJ, Vourazeris J, Myer GD, et al. The healing potential of stable juvenile osteochondritis dissecans knee lesions. *J Bone Joint Surg Am*. 2008;90:2655-2664.
47. Weiss C, Mirow S. An ultrastructural study of osteoarthritis changes in the articular cartilage of human knees. *J Bone Joint Surg Am*. 1972;54:954-972.
48. Yonetani Y, Nakamura N, Natsuume T, et al. Histological evaluation of juvenile osteochondritis dissecans of the knee: a case series. *Knee Surg Sports Traumatol Arthrosc*. 2010;18:723-730.
49. Ytrehus B, Andreas Haga H, Mellum CN, et al. Experimental ischemia of porcine growth cartilage produces lesions of osteochondrosis. *J Orthop Res*. 2004;22:1201-1209.
50. Ytrehus B, Carlson CS, Lundeheim N, et al. Vascularisation and osteochondrosis of the epiphyseal growth cartilage of the distal femur in pigs–development with age, growth rate, weight and joint shape. *Bone*. 2004;34:454-465.
51. Ytrehus B, Ekman S, Carlson CS, et al. Focal changes in blood supply during normal epiphyseal growth are central in the pathogenesis of osteochondrosis in pigs. *Bone*. 2004;35:1294-1306.
52. Ytrehus B, Grindflek E, Teige J, et al. The effect of parentage on the prevalence, severity and location of lesions of osteochondrosis in swine. *J Vet Med A Physiol Pathol Clin Med*. 2004;51:188-195.
53. Zbojniewicz AM, Stringer KF, Laor T, et al. Juvenile osteochondritis dissecans: correlation between histopathology and mri. *AJR Am J Roentgenol*. 2015;205:W114-W123.